


RESEARCH PAPER

Butyrate ameliorates caerulein-induced acute pancreatitis and associated intestinal injury by tissue-specific mechanisms

Xiaohua Pan^{1,2} | Xin Fang^{1,2,3} | Fei Wang⁴ | Hongli Li^{1,2} | Wenyong Niu^{1,2,3} |
Wenjie Liang^{1,2,3} | Chengfei Wu^{1,2} | Jiahong Li^{1,2} | Xing Tu^{1,2} | Li-Long Pan³ |
Jia Sun^{1,2} 

¹State Key Laboratory of Food Science and Technology, Jiangnan University, Wuxi, China

²School of Food Science and Technology, Jiangnan University, Wuxi, China

³School of Medicine, Jiangnan University, Wuxi, China

⁴Division of Gastroenterology and Hepatology, Digestive Disease Institute, Tongji Hospital, Tongji University School of Medicine, Shanghai, China

Correspondence

Li-Long Pan, School of Medicine, Jiangnan University, 1800 Lihu Avenue, Wuxi 214122, China.

Email: llpan@jiangnan.edu.cn

Jia Sun, State Key Laboratory of Food Science and Technology, Jiangnan University, 1800 Lihu Avenue, Wuxi 214122, China.

Email: jiasun@jiangnan.edu.cn

Funding information

Jiangsu Province Recruitment Plan for High-level, Innovative and Entrepreneurial Talents and the Fundamental Research Funds for the Central Universities, Grant/Award Numbers: JUSRP51613A, JUSRP11866; National Youth 1000 Talents Plan; Jiangsu Planned Projects for Postdoctoral Research Funds, Grant/Award Number: 2018K238C; Natural Science Foundation of Jiangsu Province, China, Grant/Award Number: BK20180619; China Postdoctoral Science Foundation, Grant/Award Number: 2018M642170; Wuxi Social Development Funds for International Science & Technology Cooperation, Grant/Award Number: WX0303B010518180007PB; National First-class Discipline Program of Food Science and Technology, Grant/Award Number: JUFSTR20180103; National Natural Science Foundation of China, Grant/Award Numbers: 31570915, 81573420, 81870439, 91642114

Background and Purpose: Acute pancreatitis (AP) is a common acute abdominal condition, frequently associated with intestinal barrier dysfunction, which aggravates AP retroactively. Butyrate exhibits anti-inflammatory effects in a variety of inflammatory diseases. However, its potential beneficial effect on AP and the underlying mechanisms have not been investigated.

Experimental Approach: Experimental AP was induced by caerulein hyperstimulation in wild-type and GPR109A^{-/-} mice. Sodium butyrate was administered intragastrically for 7 days prior to caerulein hyperstimulation. Anti-inflammatory mechanisms of butyrate were further investigated in peritoneal macrophages.

Key Results: Butyrate prophylaxis attenuated AP as shown by reduced serum amylase and lipase levels, pancreatic oedema, myeloperoxidase activity, and improved pancreatic morphology. Amelioration of pancreatic damage by butyrate was associated with reduced levels of TNF- α , IL-6, and CCL2 and suppressed activation of the NLRP3 inflammasome in both pancreas and colon. Further, butyrate ameliorated pancreatic inflammation by suppressing interactions between histone deacetylase 1 (HDAC1) and AP1 and STAT1 with increased histone acetylation at H3K9, H3K14, H3K18, and H3K27 loci, resulting in suppression of NLRP3 inflammasome activation and modulation of immune cell infiltration in pancreas. Additionally, butyrate mediated STAT1/AP1-NLRP3 inflammasome suppression via HDAC1 inhibition was demonstrated in peritoneal macrophage. In colon, butyrate inhibited NLRP3 inflammasome activation via GPR109A. Accordingly, the modulatory effects of butyrate on AP, AP-associated gut dysfunction, and NLRP3 inflammasome activation were diminished in GPR109A^{-/-} mice.

Conclusion and Implications: Our study dissected tissue-specific anti-inflammatory mechanisms of butyrate during AP, suggesting that increased colonic levels of butyrate may be a strategy to protect against AP.

Abbreviations: AP, acute pancreatitis; AP1, activator protein 1; CAE, caerulein; Co-IP, co-immunoprecipitation; DAO, diamine oxidase; HDAC, histone deacetylase; MPO, myeloperoxidase; NLRP3, nucleotide-binding domain leucine-rich repeat containing family, pyrin domain-containing 3.

Xiaohua Pan, Xin Fang, and Fei Wang contributed equally to this work.

1 | INTRODUCTION

Acute pancreatitis (AP) is an inflammatory condition of pancreas characterized by acute abdominal pain and elevation of serum pancreatic enzymes, resulting in necrosis of pancreatic acinar cell and multiorgan dysfunction. The annual global incidence of AP ranges from 13 to 45 cases per 100,000 population with the estimate of 33.74 cases per 100,000 population (Xiao et al., 2016), and the mortality rate is up to 10–15% (Uhl et al., 2002). Although its aetiology remains elusive, accumulated evidence has linked AP to inflammation of acinar cells, infiltration by innate immune cells, and derived inflammatory mediators (Watanabe, Kudo, & Strober, 2017; Zhang, Xue, Jaffee, & Habtezion, 2013). During the early stages of AP, injured acinar cells produce cytokines such as **TNF- α** , **IL-1 β** , and **IL-6** and chemokines such as **CCL2** to initiate inflammatory responses (Rodriguez-Nicolas et al., 2018). Following acinar cell damage and release of inflammatory cytokines and chemokines, neutrophils and pro-inflammatory macrophages, as the first responder cells, are recruited to the injury site and contribute to propagation of inflammatory responses and progression to severe AP (Sandler et al., 2013). Moreover, intestinal dysfunction and inflammation secondary to local pancreatic inflammation aggravate AP retroactively and is a key target to prevent systemic complications of AP (He et al., 2017). Therefore, modulation of pancreatic immune inflammatory responses and/or maintenance of gut homeostasis represent promising therapeutic approaches to alleviate AP.

Butyrate is a short-chain fatty acid produced from the fermentation of dietary fibres by intestinal microbiota (Koh, De Vadder, Kovatcheva-Datchary, & Bäckhed, 2016). Accumulating evidence has suggested that butyrate has profound effects on gut health, by suppressing intestinal inflammation and maintaining intestinal homeostasis, which is mediated by two GPCRs, **GPR41** (FFA3 receptor) and **GPR109A** (HCA₂ receptor; Singh et al., 2014). On the other hand, butyrate, acting as an inhibitor of histone deacetylases (**HDACs**), suppressed the expression of pro-inflammatory cytokines by macrophages (Chang, Hao, Offermanns, & Medzhitov, 2014), neutrophils (Vinolo et al., 2011), and dendritic cells (Arpaia et al., 2013) and also facilitates regulatory T cell generation (Arpaia et al., 2013) and M2 macrophage polarization (Ji et al., 2016). With these anti-inflammatory effects, butyrate has been evaluated in inflammatory intestinal diseases including ulcerative colitis (Vieira et al., 2012) and Crohn's disease (Laserna-Mendieta et al., 2018) and non-intestinal diseases such as Type 1 diabetes (Guo et al., 2018), mastitis (Wang et al., 2017), and neuro-inflammation (Yamawaki et al., 2018). However, the beneficial effect of butyrate on AP remains to be explored.

Here, we evaluated the protective effect of butyrate on caerulein-induced experimental AP in a mouse model. In particular, we examined the regulatory effects of butyrate on immune cell infiltration and activation, **NLRP3** inflammasome activation, and inflammatory signalling molecules key to AP in both pancreas and colon. Receptor-mediated or HDAC inhibitory mechanisms were further

What is already known

- Acute pancreatitis is associated with intestinal barrier dysfunction, which aggravates acute pancreatitis retroactively.
- Butyrate possesses immunomodulatory properties; however, its efficacy in acute pancreatitis has not been investigated.

What this study adds

- Oral administration of butyrate ameliorated acute pancreatitis and associated intestinal injury, in a mouse model.
- Butyrate attenuated acute pancreatitis by inhibiting histone deacetylase 1 in pancreas and activating GPR109A in colon.

What is the clinical significance

- Increased colonic levels of butyrate represents a novel strategy to protect against acute pancreatitis.

explored to gain insights into the anti-inflammatory action of butyrate in modulating the progression of AP.

2 | METHODS

2.1 | Animals

All animal care and experimental procedures complied with the protocols approved by the Institutional Animal Ethics Committee of Jiangnan University (JN. No 20150301-0229). Animal studies are reported in compliance with the ARRIVE guidelines (Kilkenny, Browne, Cuthill, Emerson, & Altman, 2010; McGrath & Lilley, 2015). **GPR109A^{-/-}** mice (RRID:IMSR_MUGEN:M193050) were generated by Shanghai Biomodel Organism Science & Technology Development Co., Ltd. (Shanghai, China) and crossed for more than 10 generations to a C57BL/6 background. BALB/c (RRID:IMSR_JAX:000651) or C57BL/6 (RRID:IMSR_JAX:000664) female mice (7–8 weeks old weighing 20 ± 2 g) were purchased from Su Pu Si Biotechnology Co. Ltd. (Suzhou, Jiangsu, China). Mice were housed in specific pathogen-free environment at the Animals Housing Unit of Jiangnan University (Wuxi, Jiangsu, China) with controlled temperature (24 ± 1°C) and 12-hr light–dark cycle and had free access to water and standard chow (AIN93G).

2.2 | Experimental design and animal treatments

In the present study, animals were assigned to different experimental groups of equal size in a blinded and random fashion according to the

guidelines of the *BJP*. Caerulein hyperstimulation in mice was used to induce experimental AP, as this is the most common model (Gorelick & Lerch, 2017; He et al., 2017; Pan, Li, Shamoan, Bhatia, & Sun, 2017). BALB/c mice were divided randomly into experimental groups ($n = 8$) as follows: PBS-treated control group (CON), caerulein-induced AP group (CAE), and sodium butyrate-treated groups at a dose of 50 and 200 mg·kg⁻¹ (SB + CAE). Sodium butyrate (Sigma-Aldrich, Saint Louis, MO, USA) was administered intragastrically for 7 days prior to caerulein injection. For the CON and CAE groups, mice were given equal volumes of PBS for 7 days before the first caerulein challenge. Then all mice were given hourly intraperitoneal injection of PBS or PBS-containing caerulein (50 µg·kg⁻¹ body weight) for 10 hr. One hour after the last caerulein injection, mice were killed by a lethal dose of pentobarbital sodium (90 mg·kg⁻¹; Sigma-Aldrich), and plasma, pancreatic and colonic tissue samples were collected for subsequent histopathology, enzymes and cytokine assays, immunoblotting, and flow cytometry assays. For the measurement of butyrate in blood, pancreas, and colon, a separate experiment with the same treatment design was conducted, where blood, pancreas, and colon samples were collected at 2 hr after intragastric administration of butyrate and the first caerulein injection on Day 7.

In addition, to confirm the potential role of GPR109A on AP attenuation, wild-type C57BL/6 and GPR109A^{-/-} female mice were also subjected to caerulein hyperstimulation and sodium butyrate treatment in another experiment with the same design, that is, wild-type and GPR109A^{-/-} mice were given sodium butyrate or PBS for 7 days and then given hourly intraperitoneal injection of caerulein for 10 hr to induce AP.

2.3 | Isolation and treatment of primary peritoneal macrophage

Primary peritoneal macrophages were isolated according to Maehara et al. (2015). Briefly, mice were anaesthetized with 30 mg·kg⁻¹ of pentobarbitone sodium, and then the peritoneal cavity was flushed with 5 ml of PBS, and peritoneal lavage fluids were centrifuged at 250 × *g* for 5 min at 4°C. After centrifugation, the pellet was resuspended in RPMI 1640 medium (Hyclone Laboratories, Logan, UT) supplemented with 10% fetal calf serum L-glutamine (2 mM), glucose (4.5 g·L⁻¹), and HEPES buffer (10 mM), in the presence of 100 mg·ml⁻¹ streptomycin and 100 U·ml⁻¹ penicillin (PAA). The cells (2×10^6) were seeded in six-well plates at 37°C under a 5% CO₂ atmosphere for 2 hr and washed twice with PBS. The suspended cells were then removed and the adherent cells were collected as peritoneal macrophages. Thereafter, macrophages were cultured with fresh RPMI 1640 medium in the absence or presence of sodium butyrate (5 µM, 100 µM, and 2 mM) for 24 hr and then stimulated with 100 ng·ml⁻¹ LPS (*Escherichia coli* serotype O111:B4, Sigma) for 6 hr; then cells were collected for immunoblotting analysis. The time point (6 hr) for LPS treatment was selected according to preliminary experiments (Figure S1).

2.4 | Butyrate measurement

The concentrations of butyrate in blood, pancreas, and colon were measured by GC coupled to the MS detector of GCMS-QP2010 (Shimadzu, Japan) as described previously (Sun et al., 2015). Briefly, whole colonic and pancreatic tissue samples were weighed into 1.5-ml tubes and homogenized with 500 µl of saturated NaCl solution. Subsequently, samples were deproteinated with 40 µl of 10% sulfuric acid, and diethyl ether (1 ml) was added to extract butyrate. Samples were then centrifuged at 14,000 × *g* for 15 min at 4°C, and supernatants were used for the analysis of butyrate. Supernatants of 1 µl were injected into Rtx-WAX capillary column (30 m × 0.25 mm × 0.25 µm, Bellefonte, PA, USA) installed on the GC and coupled to the MS detector of GCMS-QP2010 (Shimadzu, Japan). For serum butyrate measurement, 16 µl of sulfuric acid and 400 µl of diethyl ether were added to 200 µl of serum samples. Tubes were vortexed and centrifuged as previously described, and 1 µl was injected into the gas chromatograph.

To quantify butyrate, a calibration curve for the concentration range of 0.014–1.135 mM was constructed. Butyrate measurement was performed following our previous protocol (Sun et al., 2015): The initial oven temperature was 100°C and increased to 140°C at a rate of 7.5°C·min⁻¹. The temperature was further increased to 200°C at a rate of 60°C·min⁻¹ and remained for 3 min. Helium was utilized as the carrier gas at a flow rate of 0.89 ml·min⁻¹, and the column head pressure was 62.7 kPa. The injector was set at 240°C. The injection mode was split, and the ratio was 10:1. For mass spectrometer, ion source temperature was 220°C, interface temperature was 250°C, and the scan range was from *m/z* 2 to 100. Real-time analysis software GCMS Postrun (GCMS solution Version 2.72) was employed to compare the relative concentrations of butyrate.

2.5 | Measurement of serum diamine oxidase, amylase, and lipase activities

Fresh blood was collected and centrifuged at 3,000 × *g* for 15 min at room temperature. The supernatant was then collected and stored at -80°C until analysis. Serum diamine oxidase (DAO) activity was analysed using a commercial kit (A088-1; Jiancheng Bioengineering Institute, Nanjing, Jiangsu, China). Serum amylase activity was determined using an iodine-starch colorimetric method by an assay kit (C016; Jiancheng Bioengineering Institute). Serum lipase activity was measured using a turbidometric assay (A054-2; Jiancheng Bioengineering Institute).

2.6 | Determination of pancreatic oedema

Pancreatic oedema was quantified by the wet weight to dry weight ratio. The initial weight of the freshly excised pancreas was defined as the wet weight. The weight of the same sample after desiccation at 60°C for 72 hr served as the dry weight.

2.7 | Determination of myeloperoxidase activity in pancreas

Myeloperoxidase (MPO) activity was evaluated using an MPO assay kit (A044; Jiancheng Bioengineering Institute) according to the manufacturer's protocol as previously described (Sun et al., 2017). Pancreatic tissues were homogenized (IKA homogenizer, Staufen, Germany) in 0.9% saline. Five percent of pancreatic tissue homogenates (200 μ l) and chromogenic reagent (3 ml) were added to a sterile tube, and after mixing, was incubated in a water bath for 30 min at 37°C. Stop solution (provided by the assay kit) was added to end the reaction. Absorbance was then analysed at 460 nm within 10 min, and MPO activities are expressed as units per gram tissue.

2.8 | Histopathological examination

Fresh pancreatic and colonic samples were fixed with 4% paraformaldehyde overnight, washed with running water for 2 hr, dehydrated with a gradient of ethanol, and then embedded in paraffin and cut into 5- μ m sections. The sections were dewaxed in xylene, hydrated through upgraded ethanol solutions and stained with haematoxylin and eosin. Pancreatic and lung damage were assessed under a DM2000 light microscope (Leica Microsystems GmbH, Wetzlar, Germany) at 200 \times magnification.

2.9 | Cytokine assays

ELISA was employed to assay the levels of TNF- α , IL-6, and CCL2 in the tissues and serum. Specifically, pancreas and colon samples were homogenized in 20-mM phosphate buffer (pH 7.4) and centrifuged at 10,000 \times g for 15 min at 4°C. The supernatants were used for measuring tissue levels of inflammatory mediators. Serum prepared by centrifugation of blood samples was used for measuring circulating levels of inflammatory mediators.

The TNF- α (MTA00B), IL-6 (M6000B), and MCP-1 (MJE00) levels in serum and pancreatic and colonic tissues were assayed by ELISAs using commercially available kits (R&D Systems, Minneapolis, MN, USA) according to the manufacturer's instructions. Specifically, pancreas and colon samples were homogenized in 20-mM phosphate buffer (pH 7.4) and centrifuged at 10,000 \times g for 15 min at 4°C; the supernatants were collected for measurement of tissue cytokines. The OD was measured using a spectrophotometer at 450 nm with a correction wavelength set at 570 nm.

2.10 | Immunoblotting

All immunoblotting procedures and analysis complied with BJP guidelines (Alexander et al., 2018). Pancreas and colon samples were homogenized in ice-cold lysis RIPA buffer (P0013B; Beyotime Biotechnology, Shanghai, China; containing protease inhibitors and

phosphatase inhibitors) and centrifuged at 10,000 \times g for 15 min at 4°C. Protein concentration was quantified using a BCA protein assay kit (P0010; Beyotime Biotechnology). Equal amounts of protein were separated by electrophoresis in SDS-PAGEs and then transferred onto polyvinylidene difluoride membranes (Millipore, USA). The membranes were blocked with 5% non-fat milk (w/v) in 0.05% Tris-buffered saline with Tween for 2 hr at room temperature and then incubated with respective primary antibodies overnight at 4°C. After being washed with Tris-buffered saline with Tween, the membranes were incubated with respective secondary antibodies at a dilution of 1:5,000 for 2 hr at room temperature. Primary antibodies against **HDAC1** (Cat#5356S, 1:1,000, RRID:AB_10612242), **HDAC2** (Cat#2540S, 1:1,000, RRID:AB_2116822), **HDAC3** (Cat#3949T, 1:1,000, RRID:AB_2118371), Ac-H3K14 (Cat#7627T, 1:1,000, RRID:AB_10839410), Ac-H3K18 (Cat#9675, 1:2,000, RRID:AB_331550), Ac-H3K27 (Cat#14056; 1:1,000, RRID:AB_2798379), Ac-H3K56 (Cat#4243, 1:1,000, RRID:AB_10548193), Histone 3 (Cat#14269, 1:1,000, RRID:AB_2756816), NLRP3 (Cat#15101S, 1:500, RRID:AB_2722591), ASC (Cat#67824S, 1:1,000, RRID:AB_2799736), STAT1 (Cat#14994S, 1:1,000, RRID:AB_2737027), p-NF- κ B p65 (Cat#3033S, 1:1,000, RRID:AB_331284), and IL-1 β (Cat#52718S, 1:1,000, RRID:AB_2799421) were purchased from Cell Signaling Technology (Boston MA, USA). Antibodies for Ac-H3K9 (Cat#ab10812, 1:500, RRID:AB_297491), STAT3 (Cat#ab68153, 1:2,000), IL-18 (Cat#ab71495, 1 μ g·ml⁻¹, RRID:AB_1209302), AP1 (Cat#ab32137, 1:2,000, RRID:AB_731608), p-AP1 (Cat#ab32385, 1:5,000, RRID:AB_726900), NF- κ B p65 (Cat#ab16502, 0.5 μ g·ml⁻¹, RRID:AB_2224674), p-STAT1 (Cat#ab109461, 1:5,000, RRID:AB_10863745), and p-STAT3 (Cat#ab76315, 1:10,000, RRID:AB_1658549) were purchased from Abcam (Cambridge, MA, USA). Antibodies against Caspase-1 p20 (Cat#sc-398715, 1:500) and GAPDH (Cat#sc-32233, 1:5,000, RRID:AB_627679) were purchased from Santa Cruz Biotechnology (Santa Cruz, CA, USA). Antibodies for GPR41 (Cat#BS5750, 1:500) and GPR109A (Cat#BS2605, 1:500) were purchased from Bioworld Technology (Louis Park, MN, USA). The proteins were visualized by Plus-enhanced chemiluminescence using FluorChem FC3 (ProteinSimple, CA, USA). The densitometric analyses of protein expression by immunoblotting were performed by AlphaView Software (ProteinSimple). GAPDH was adopted as internal standard to control for unwanted sources of variation, and relative protein expression values were expressed as "fold mean of the controls" by comparing to the corresponding control value, and the control value was normalized to 1.0.

2.11 | Co-immunoprecipitation

Whole-cell lysates were prepared using a RIPA buffer (Beyotime, Shanghai) containing protease and phosphatase inhibitors followed by 15 min centrifugation at 10,000 \times g at 4°C. For co-immunoprecipitation (Co-IP), 200 μ g of the crude whole-cell extract was incubated with 2 μ g of anti-HDAC1 (Santa Cruz Biotechnology) at 4°C overnight. Then 20 μ l of prewashed protein A/G agarose

(Santa Cruz Biotechnology) was added to the mixture and incubated at 4°C for 3 hr with gentle agitation. After extensive washing with RIPA buffer, HDAC1-interacting proteins were eluted with SDS buffer and analysed by immunoblotting.

2.12 | Flow cytometry

Freshly excised pancreatic tissues were digested in 0.75 mg·ml⁻¹ collagenase-P solution (Roche Basel, Switzerland) at 37°C for 15 min. The digested pancreatic pieces were subsequently dissociated with gentle MACS Dissociator (Miltenyi Biotechnology, Bergisch Gladbach, NRW, Germany) and filtered through 75-µm filter screens with PBS immediately. Single cell suspensions were stained with several monoclonal antibodies for 15 min at room temperature. For neutrophil determination, cells were surface stained with PE/Cy7 anti-mouse CD45, Alexa Fluor 488 anti-mouse F4/80, Brilliant Violet 421 anti-mouse/human CD11b, and Alexa Fluor 647 anti-mouse Ly6G from BioLegend (San Diego, CA, USA). For macrophages, cells were fixed and permeabilized by employed Cell Fixation & Permeabilization Kit after surface stained with anti-CD45, anti-CD11b, and anti-F4/80 and subsequently stained with PE anti-mouse CD206 (BioLegend). Stained cells were analysed on Attune NxT (Thermo Fisher Scientific, Waltham, MA, USA).

2.13 | Data and statistical analysis

The data and statistical analysis comply with the recommendations on experimental design and analysis in pharmacology (Curtis et al., 2018). All data were analysed blindly using GraphPad Prism 7 software (RRID:SCR_002798; San Diego, CA, USA), and data are shown as mean ± SEM. For immunoblotting, data were normalized to the mean values of the control group to reduce unwanted sources of variation. The group size for data subjected to statistical analysis was $n \geq 6$, where n is the number of mice in each group or the number of separate experiments (in vitro), and statistical analysis was done using these biological replicates. The distribution of the data was tested with the Shapiro–Wilk normality test. Outliers were tested using Grubb's test. Homogeneity of the variances was checked by Levene's test. Statistical significance between groups was evaluated with one-way ANOVA followed by Tukey's post hoc test. For all one-way ANOVAs, post hoc tests were run only if F achieved $P < .05$ and there was no significant variance inhomogeneity. For preliminary immunoblotting data in Figure S1 for selecting the optimal time point, no statistical analysis was performed owing to group size of $n < 5$. Statistical significance was set at $P < .05$.

2.14 | Nomenclature of targets and ligands

Key protein targets and ligands in this article are hyperlinked to corresponding entries in <http://www.guidetopharmacology.org>, the

common portal for data from the IUPHAR/BPS Guide to PHARMACOLOGY (Harding et al., 2018), and are permanently archived in the Concise Guide to PHARMACOLOGY 2017/18 (Alexander, Christopoulos et al., 2017; Alexander, Fabbro et al., 2017; Alexander, Kelly et al., 2017).

3 | RESULTS

3.1 | Butyrate prophylaxis mitigates the severity of AP

We have examined the effects of butyrate on the most widely used model of AP, induced by caerulein hyperstimulation in mice. Compared with untreated mice with AP, pre-treatment with sodium butyrate (200 mg·kg⁻¹) clearly decreased the severity of AP, as shown by reduced serum amylase and lipase activities, pancreatic oedema, and pancreatic MPO activities (Figure 1a–d), along with reduction of AP-associated lung injury (Figure S2). Histological examination of pancreatic tissues further confirmed a protective effect of sodium butyrate at this dose, shown by improved cellular morphology, pancreatic oedema, reduced inflammatory cell infiltration, and acinar necrosis (Figure 1e). The pro-inflammatory cytokine production is an early pathological feature of AP, and sodium butyrate reduced AP-caused increases in pancreatic TNF-α, CCL2, and IL-6 levels (Figure 1f). Further GC–MS measurements found that mice treated with 200 mg·kg⁻¹ sodium butyrate had measurable butyrate levels in colon (0.65 µmol·g⁻¹), serum (99.76 µM), and pancreas (0.16 µmol·g⁻¹), all significantly higher than those in the CON and CAE groups (Figure 1g).

3.2 | Butyrate modulates innate immune cell responses during AP

The dysregulated infiltration of innate immune cells, including neutrophils and macrophages, are key pathophysiological agents in AP development. Therefore, we determined the proportion of neutrophils (CD45⁺CD11b⁺Ly6G⁺) and of macrophages (CD45⁺CD11b⁺F4/80⁺) in pancreas of AP mice. As shown in Figure 2, AP induction was accompanied by robust increases of infiltrating macrophages (Figure 2a) and neutrophils (Figure 2c). Treatment with sodium butyrate decreased the total number of macrophages in pancreas (Figure 2a) and promoted macrophage polarization to the anti-inflammatory M2 macrophages (CD45⁺CD11b⁺F4/80⁺CD206⁺; Figure 2b). In addition, sodium butyrate markedly attenuated the infiltration of neutrophils in pancreas (Figure 2c).

3.3 | Butyrate attenuates AP-associated intestinal injury

The dysregulated gut homeostasis, marked by intestinal damage and inflammation, further aggravates AP. Next, we evaluated whether

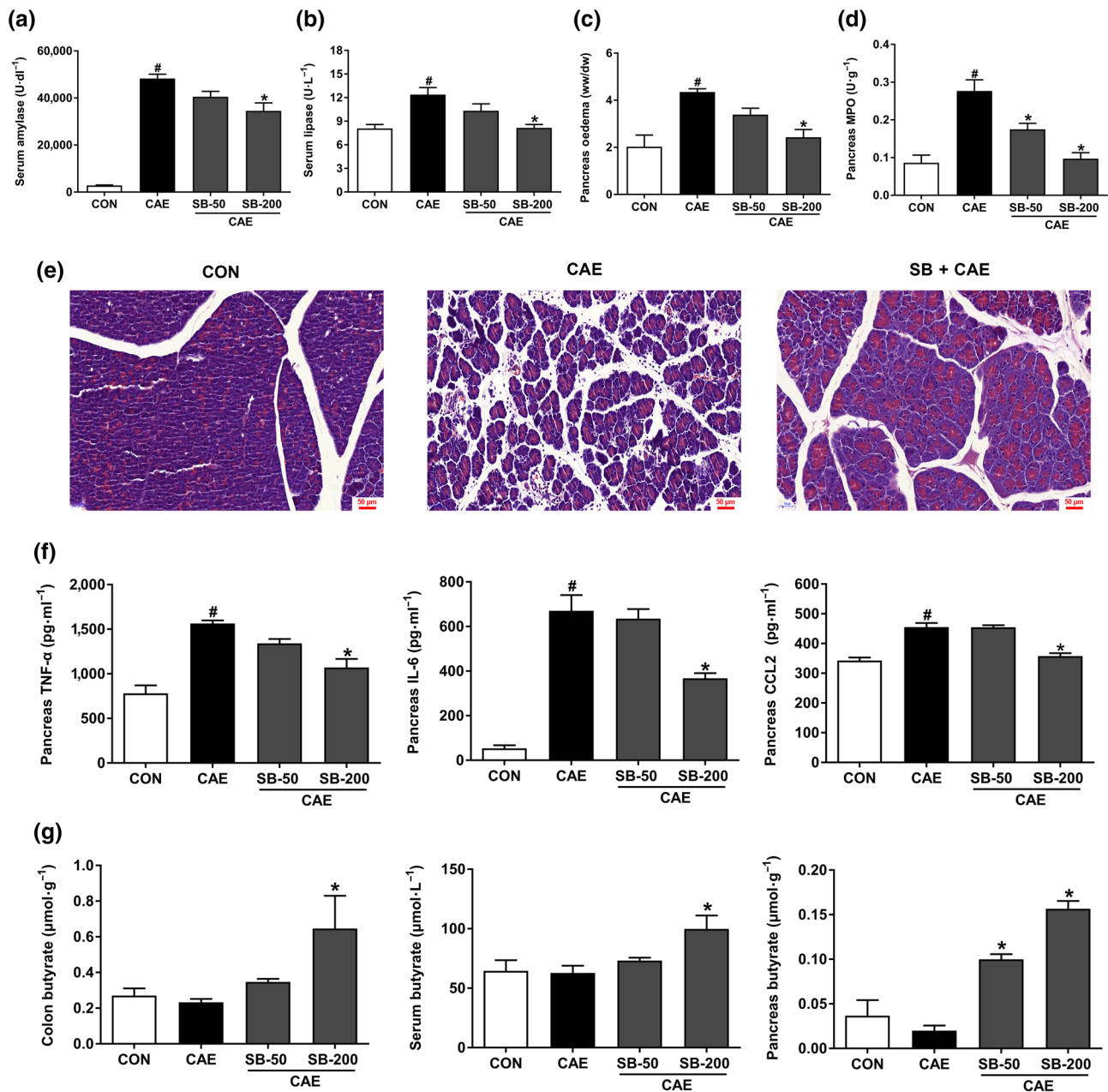


FIGURE 1 Prophylactic treatment with oral butyrate mitigates the severity of AP. Mice were challenged with PBS (CON), caerulein (CAE), or 50 and 200 mg·kg⁻¹ sodium butyrate combined with caerulein (SB + CAE). Levels of serum amylase (a) and lipase (b), pancreatic oedema (c), and myeloperoxidase (MPO) activity (d) in pancreas. (e) Representative histopathological sections of pancreatic tissues by haematoxylin–eosin staining. Scale bar: 50 μm. (f) ELISA analyses of TNF-α, IL-6, and CCL2 levels in pancreas. (g) GC-MS detection of butyrate levels in colon, serum, and pancreas. Data shown are means ± SEM, n = 8. #P < .05, significantly different from CON; *P < .05, significantly different from CAE; one-way ANOVA followed by Tukey's post hoc test

pre-treatment with sodium butyrate maintained intestinal homeostasis and thus attenuated AP development. Histological examination of colonic tissue revealed that sodium butyrate reversed the reduction of colonic villus length during AP induction (Figure 3a,b). In addition, butyrate ameliorated AP-associated intestinal inflammation and injury as shown by the reduced levels of intestinal pro-inflammatory cytokines, including TNF-α, CCL2, and IL-6 (Figure 3c). Meanwhile, butyrate improved gut barrier function, as shown by the lower levels of serum DAO, compared with those in AP mice (Figure 3d).

3.4 | Butyrate decreases pancreatic and colonic NLRP3 inflammasome activation

The NLRP3 inflammasome is an intracellular multiprotein complex triggering inflammatory responses. Next, we assessed the effect of sodium butyrate on the activation of NLRP3 inflammasome in pancreas and colon. As shown in Figure 4, caerulein stimulated the expression of NLRP3, ASC, caspase-1 (p20), and its downstream cytokines cleaved-IL-1β and cleaved-IL-18 in both

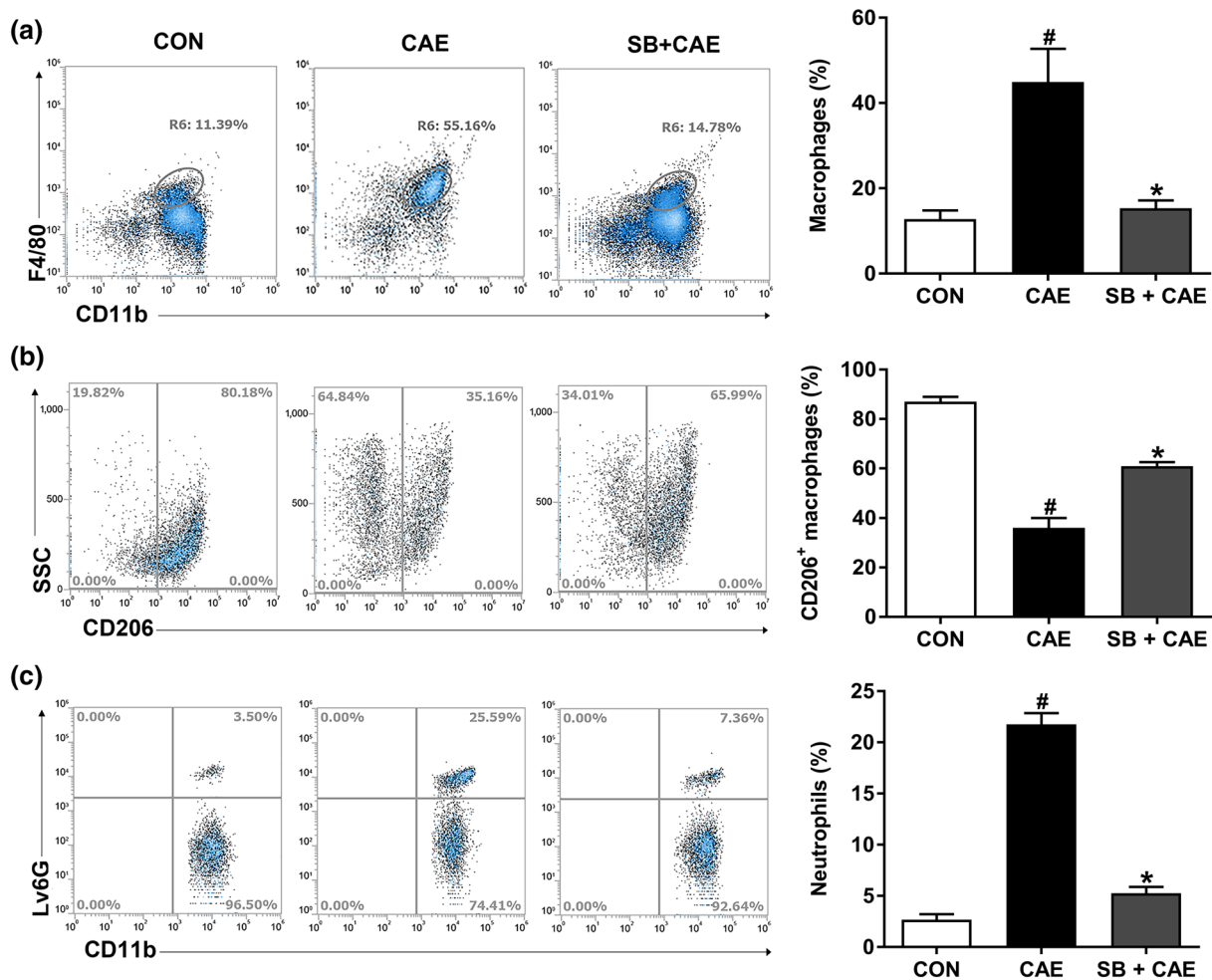


FIGURE 2 Butyrate prophylaxis decreases innate immune cell infiltration into pancreas during AP. Mice were challenged with PBS (CON), caerulein (CAE), or 200 mg·kg⁻¹ sodium butyrate combined with caerulein (SB + CAE). The frequency of (a) total macrophages (CD45⁺CD11b⁺F4/80⁺), (b) M2 macrophages (CD45⁺CD11b⁺F4/80⁺CD206⁺), and (c) neutrophils (CD45⁺CD11b⁺Ly6G⁺) in pancreas was detected by flow cytometry. Data shown are means ± SEM, *n* = 6. #*P* < .05, significantly different from CON; **P* < .05, significantly different from CAE; one-way ANOVA followed by Tukey's post hoc test

pancreas (Figure 4a) and colon (Figure 4b). These results showed that pre-treatment with sodium butyrate markedly suppressed the expression of NLRP3 and associated proteins, suggesting that the anti-inflammatory effects of butyrate were associated with inhibited NLRP3 inflammasome activation.

3.5 | Butyrate blocks AP-activated transcription factors

Activation of NLRP3 inflammasome during AP is regulated by a number of transcription factors including NF-κB, AP1, and STAT3 (Gukovskaya, Gukovsky, Algul, & Habtezion, 2017). We next analysed the modulatory effects of butyrate on activation of inflammation-triggering transcription factors in pancreas and colon. As shown in Figure 5, the phosphorylation of AP1, STAT1, and STAT3 in pancreas was significantly suppressed by sodium butyrate treatment (Figure 5a). In contrast, the phosphorylation of NF-κB p65 and AP1,

but not STAT1 or STAT3, was decreased in colon by sodium butyrate treatment (Figure 5b).

3.6 | Butyrate regulates the interaction between HDAC1 and AP1, and STAT1 in pancreas

Previous studies have demonstrated that butyrate attenuates inflammation by inhibiting HDAC activity (Chang et al., 2014; Chen et al., 2018). Our results showed that sodium butyrate selectively suppressed HDAC1 but not HDAC2 or HDAC3 in the pancreas (Figure 6a) and colon (Figure 6b). HDAC1 suppression was accompanied by increased histone acetylation at H3K9, H3K14, H3K18, and H3K27 loci in the pancreas (Figure 6c), while these acetylation sites of histone 3 remained unaltered in the colon (Figure 6d). HDAC inhibition may regulate downstream targets such as NF-κB (Leus, Zwinderman, & Dekker, 2016), AP1 (Sanna & Galeotti, 2018), STAT1 (Ginter et al., 2012), and STAT3 (Xiong et al.,

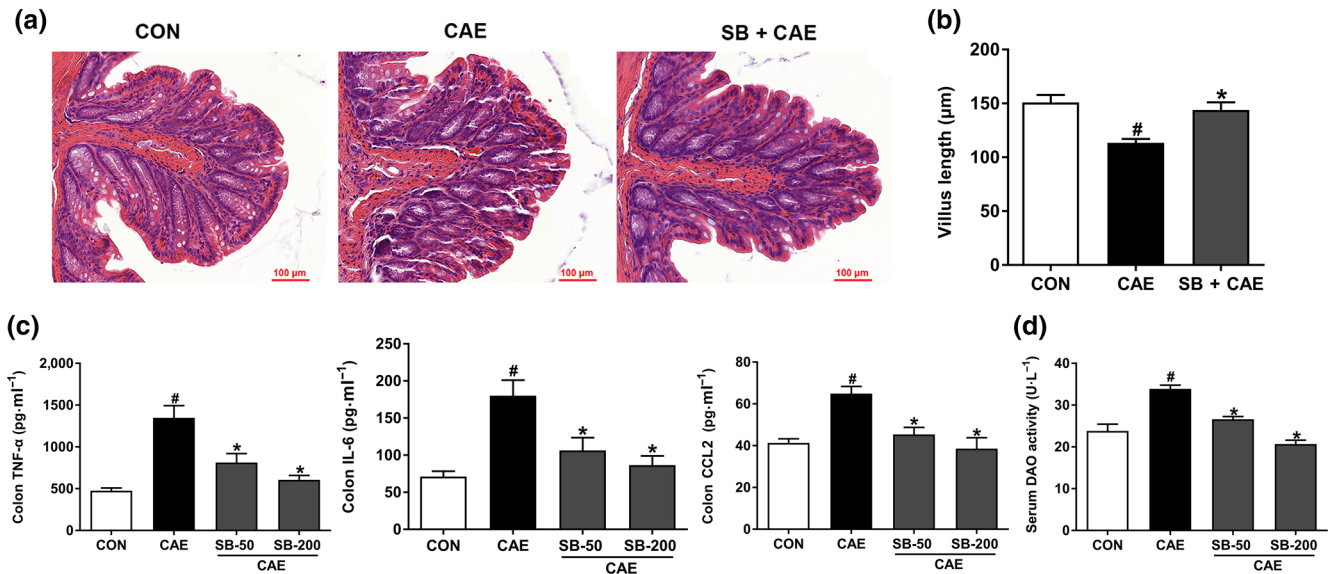


FIGURE 3 Butyrate attenuates AP-associated colon injury. Mice were challenged with PBS (CON), caerulein (CAE), or 50 and 200 mg·kg⁻¹ sodium butyrate combined with caerulein (SB + CAE). (a) Representative histopathological sections of colon by haematoxylin–eosin staining. Scale bar: 100 μm. (b) Colonic crypt length. (c) ELISA detection of TNF-α, IL-6, and CCL2 levels in colon. (d) Serum diamine oxidase (DAO) activity. Data shown are means ± SEM, n = 8. #P < .05, significantly different from CON; *P < .05, significantly different from CAE; one-way ANOVA followed by Tukey's post hoc test

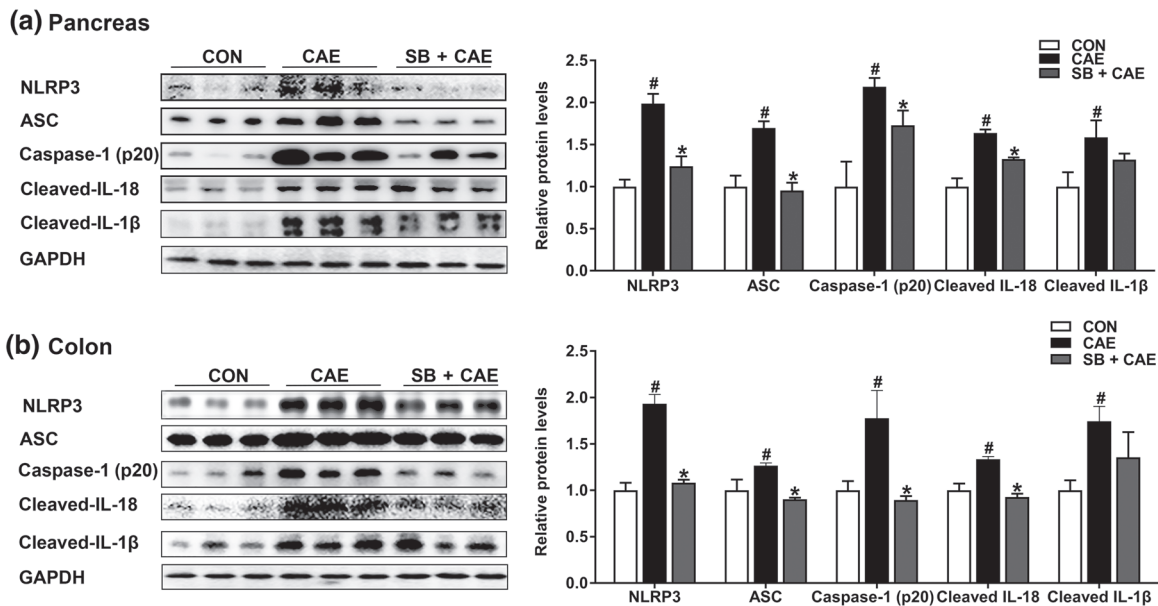
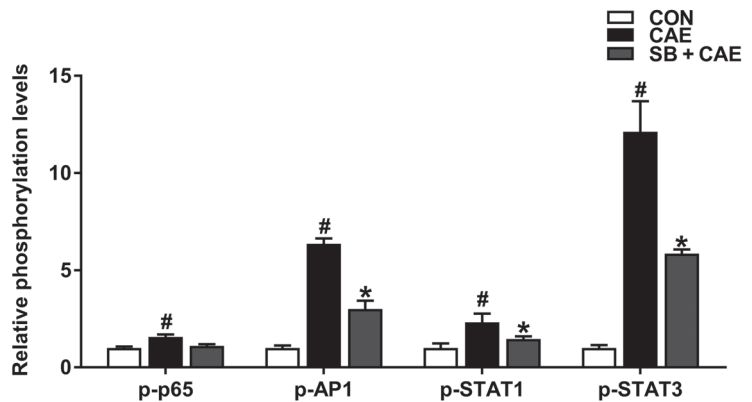
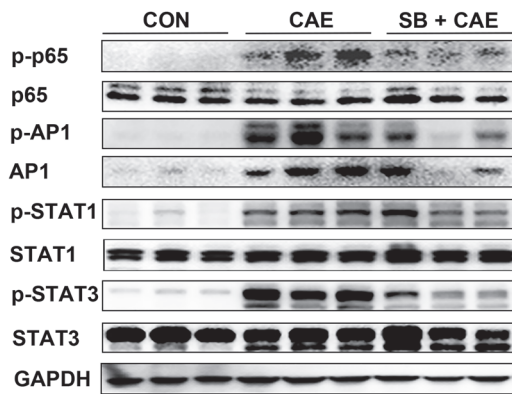


FIGURE 4 Butyrate attenuates pancreatic and colonic injury and inflammatory response by modulating NLRP3 inflammasome pathway. Mice were challenged with PBS (CON), caerulein (CAE), or 200 mg·kg⁻¹ sodium butyrate combined with caerulein (SB + CAE). Representative bands of Western blot and quantitative analyses of NLRP3 inflammasome pathway in pancreas (a) and colon (b). Data shown are means ± SEM, n = 8. #P < .05, significantly different from CON; *P < .05, significantly different from CAE

2012) in different contexts. By further immunoprecipitation analysis, we observed that HDAC1 was coimmunoprecipitated with AP1 and STAT1 in the pancreas during AP, and the interactions were inhibited by sodium butyrate (Figure 6e). HDAC1 interacted with STAT1 and STAT3 similarly in colon during AP, which, however, was not affected by sodium butyrate treatment (Figure 6f).

To be noted, effects of sodium butyrate were found comparable to those of a well-characterized HDAC inhibitor, [suberoylanilide hydroxamic acid \(vorinostat; 50 mg·kg⁻¹\)](#) in HDAC1 inhibition and attenuation of pancreatic damage and inflammation (Figure S3). In addition, sodium butyrate but not suberoylanilide hydroxamic acid significantly reduced pancreatic oedema (Figure S3). Furthermore,

(a) Pancreas



(b) Colon

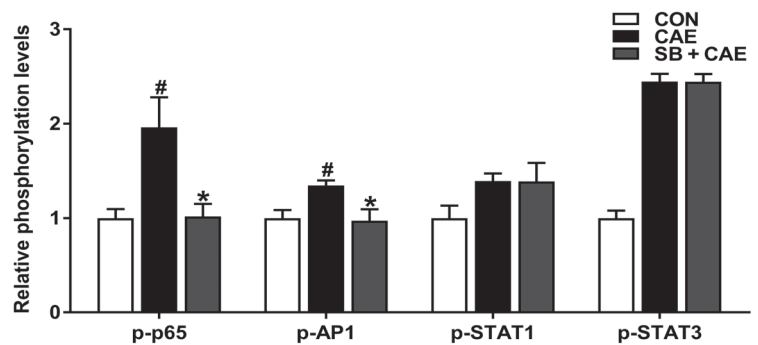
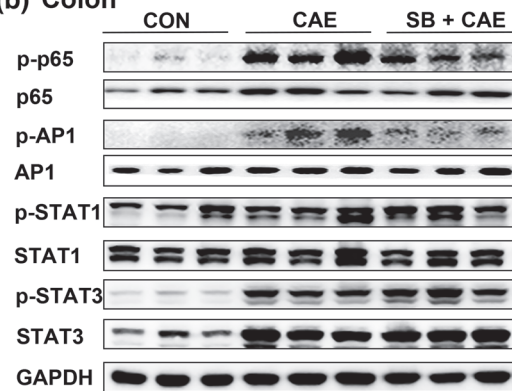


FIGURE 5 Butyrate blocks the activation of transcription factors. Mice were challenged with PBS (CON), caerulein (CAE), or 200 mg·kg⁻¹ sodium butyrate combined with caerulein (SB + CAE). Representative bands of Western blot and phosphorylation quantification of transcription factors NF- κ B, AP1, STAT1, and STAT3 in pancreas (a) and colons (b). Data shown are means \pm SEM, $n = 8$. [#] $P < .05$, significantly different from CON; ^{*} $P < .05$, significantly different from CAE; one-way ANOVA followed by Tukey's post hoc test

in peritoneal macrophages stimulated by LPS (100 ng·ml⁻¹, 6 hr, based upon preliminary experiments in Figure S1), sodium butyrate suppressed, in a dose-dependent manner, HDAC1, phosphorylation of AP1 and STAT1 and downstream activation of NLRP3 and associated proteins (Figure 7). Together, these results demonstrate that butyrate exerts its anti-inflammatory effects via inhibiting HDAC1 activity in pancreas but not in colon.

3.7 | Butyrate protects against AP via its receptor GPR109A in colon

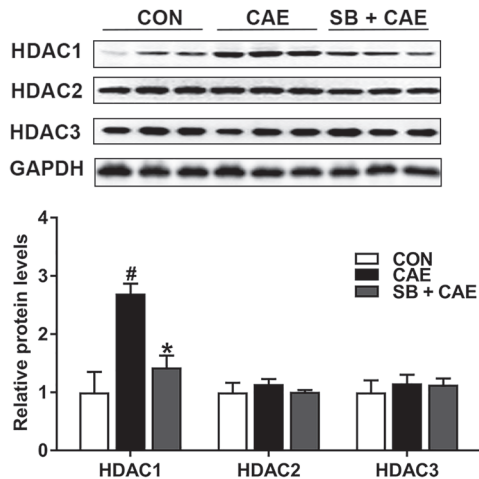
As the acetylation sites of histone and interaction between HDAC1 and transcription factors in the colon were not altered by butyrate, we went on to determine whether the beneficial effects of butyrate on the colon were mediated via the known receptors for butyrate, GPR109A and GPR41. As shown in Figure 8, the expression of GPR109A but not GPR41, in the colon was significantly up-regulated by sodium butyrate treatment in mice (Figure 8a), while its expression in the pancreas was unchanged (Figure 8b). These results suggested that butyrate may exert anti-inflammatory effects by activating GPR109A in the colon.

To confirm a receptor-mediated effect in the gut, we compared the effects of sodium butyrate administration on the severity of AP in wild-type and GPR109A^{-/-} mice. We found that the protective effects of sodium butyrate on AP were diminished in GPR109A^{-/-} mice (Figure 8c-f). Compared to wild-type mice, GPR109A^{-/-} mice had higher serum DAO levels (Figure 8g) and enhanced activation of NLRP3 inflammasome in colon (Figure 8i). Consistently, the absence of GPR109A in mice blocked the inhibitory effects of sodium butyrate on serum DAO release (Figure 8g) and canonical NLRP3 inflammasome mediated caspase 1 activation and resultant IL-1 β and IL-18 production in colon. In pancreas, such effects were only partly observed, confirming a tissue-specific mechanism of butyrate (Figure 8h,i). These data together pointed to a role for GPR109A in mediating intestinal homeostasis by butyrate, and thus to attenuate AP.

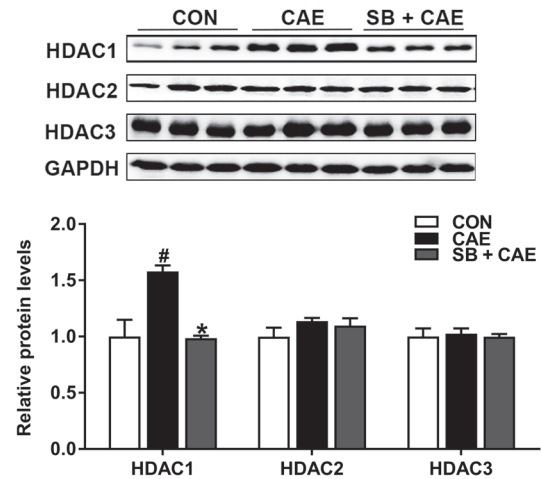
4 | DISCUSSION

In the present study, we have demonstrated that butyrate displayed multifaceted protective effects against caerulein-induced AP in mice by attenuating pancreatic oedema and acinar necrosis, preventing the

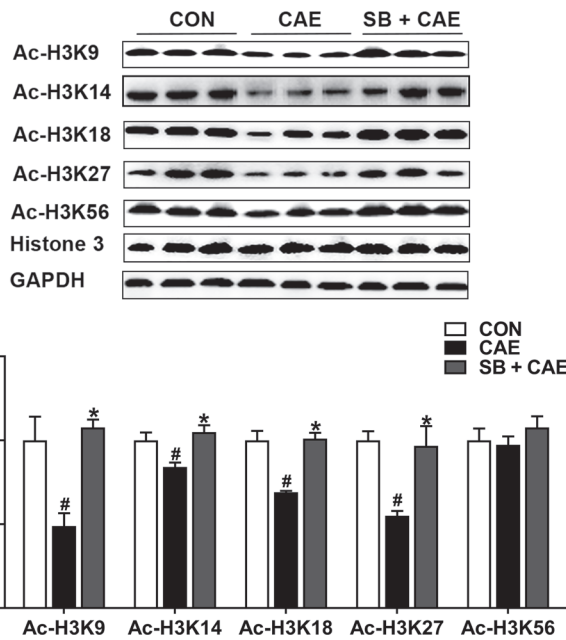
(a) Pancreas



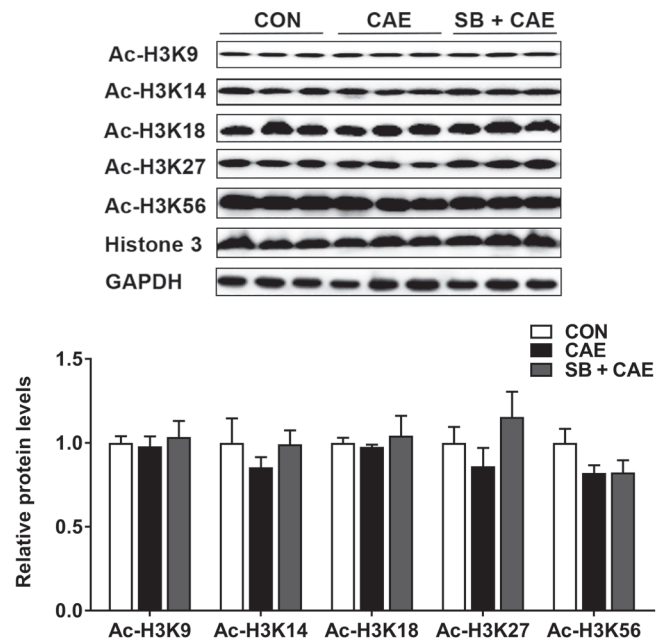
(b) Colon



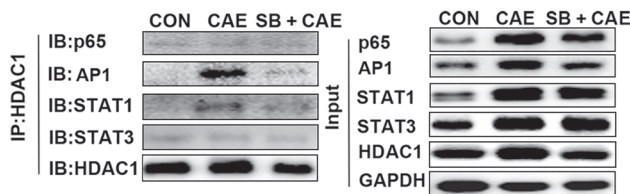
(c) Pancreas



(d) Colon



(e) Pancreas



(f) Colon

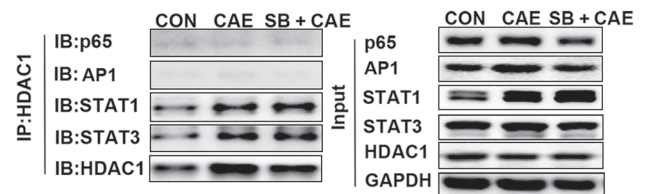


FIGURE 6 Butyrate exerts anti-inflammatory effects by acting as HDAC inhibitor in the pancreas but not in colon. Mice were challenged with PBS (CON), caerulein (CAE), or 200 mg·kg⁻¹ sodium butyrate combined with caerulein (SB + CAE). Protein expression of HDAC1, 2, and 3 in pancreas (a) and colon (c) was determined by Western blot. Histone acetylation at H3K9, H3K14, H3K18, H3K27, and H3K56 in pancreas (b) and colon (d) was detected by Western blot. Co-IP analysis of HDAC1 with NF-κB (p65), AP1, STAT1, and STAT3 in pancreas (e) and colon (f). Data shown are means ± SEM, n = 8. [#]P < .05, significantly different from CON; ^{*}P < .05, significantly different from CAE; one-way ANOVA followed by Tukey's post hoc test

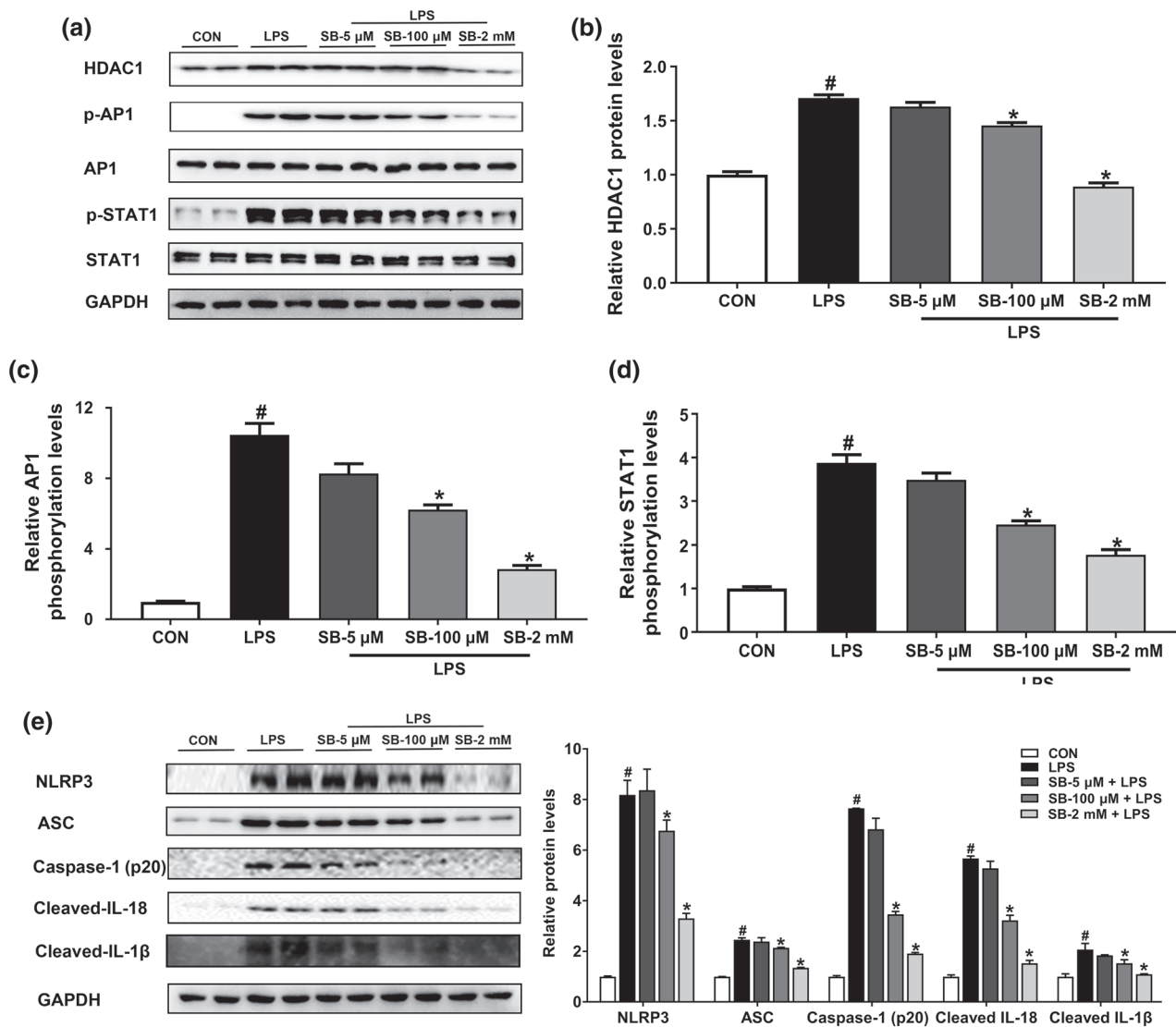


FIGURE 7 Butyrate inhibits AP1/STAT1 phosphorylation and NLRP3 inflammasome activation by acting as an HDAC1 inhibitor in peritoneal macrophage. Cells were pretreated with sodium butyrate (SB; 5 μ M, 100 μ M, and 2 mM) for 24 hr followed by incubation with 100 ng·ml⁻¹ LPS for 6 hr. (a) Representative bands of Western blot. (b) Relative quantitative analyses of HDAC1 expression in macrophages. (c, d) Phosphorylation analyses of transcription factors AP1 (c) and STAT1 (d) in macrophages. (e) Western blotting analysis of NLRP3 inflammasome and associated proteins' expression in macrophages. Data shown are means \pm SEM, $n = 8$. [#] $P < .05$, significantly different from CON; ^{*} $P < .05$, significantly different from LPS; one-way ANOVA followed by Tukey's post hoc test

recruitment of neutrophils and the production of pro-inflammatory cytokines in the pancreas and colon. More importantly, we demonstrated tissue-specific anti-inflammatory mechanisms of butyrate on pancreatic inflammation and associated intestinal injury, that is, butyrate acting as an HDAC1 inhibitor in pancreas or as a GPR109A agonist in colon, to suppress the activation of NLRP3 inflammasome. Meanwhile, the restored intestinal homeostasis by butyrate prophylaxis at least partially contributes to amelioration of AP.

Butyrate is known to exert anti-inflammatory and immunomodulatory effects in a variety of disease models. As a macronutrient of dairy products such as Parmigiano Reggiano cheese (1.2 g·kg⁻¹), butyrate mediated its immunonutritional effect in children with food allergy (Grimaldi et al., 2016). In addition, Lee et al. (2017) demonstrated that intragastric administration of 100 mg·kg⁻¹ of butyrate

attenuated murine colitis by blocking pro-inflammatory cytokine production in intestinal epithelial cells and macrophages, while 0.1 to 10 mg·kg⁻¹ (Chang et al., 2014) and 20 mg·kg⁻¹ (Lee et al., 2017) of butyrate were not effective. Furthermore, administration of butyrate (50, 100, and 200 mg·kg⁻¹) protected against mouse mastitis in a dose-dependent manner (Wang, Wei, et al., 2017), and treatment with butyrate (500 mg·kg⁻¹) ameliorated Type 1 diabetes (Guo et al., 2018) and lung injury (Li et al., 2018). A higher dose of 1,200 mg·kg⁻¹ of butyrate is the most frequently used dose for treating neuroinflammation in mice (Yamawaki et al., 2018). Here, we have used the most common model of AP induced by caerulein, which has proven reproducibility and is relevant to initiating mechanisms of clinical AP, in order to evaluate the prophylactic effects of butyrate (Gorelick & Lerch, 2017). We observed that administration of 200 mg·kg⁻¹ of

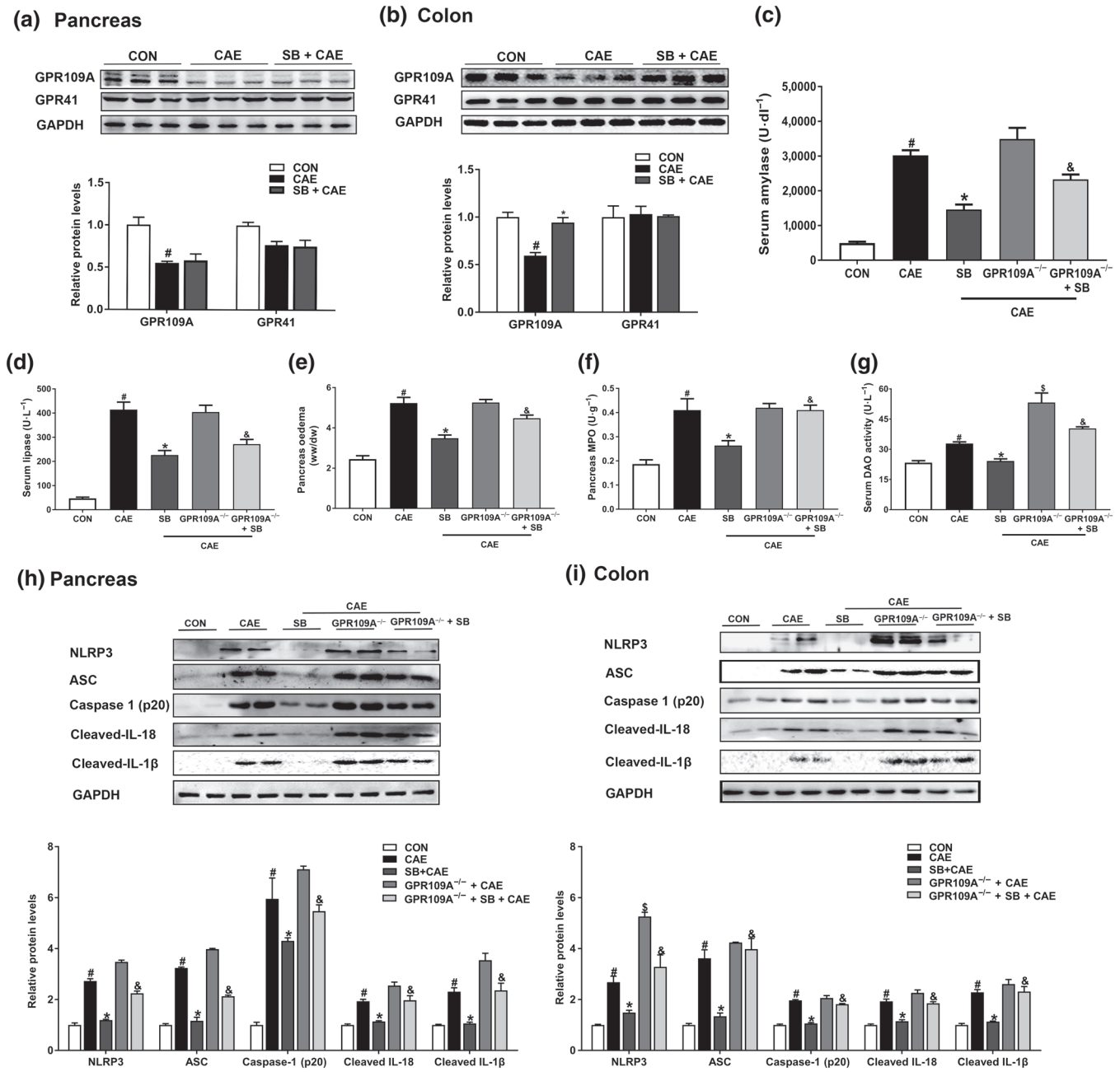


FIGURE 8 Butyrate protects against colonic inflammation via its receptors GPR109A, contributing to AP attenuation. Mice were challenged with PBS (CON), caerulein (CAE), or 200 mg·kg⁻¹ sodium butyrate combined with caerulein (SB + CAE). Western blot analysis of GPR109A and GPR41 in pancreas (a) and colon (b). Levels of serum amylase (c) and lipase (d), pancreatic oedema (e), and myeloperoxidase (MPO) activity (f) in pancreas. (g) Serum diamine oxidase (DAO) activity. Western blot analysis of NLRP3 inflammasome and associated protein expression in pancreas (h) and colon (i), and values represented fold change after normalization to control. Data shown are means ± SEM, n = 8. [#]P < .05, significantly different from CON; ^{*}P < .05, significantly different from CAE; [§]P < .05, significantly different from CAE; [&]P < .05, significantly different from SB + CAE; one-way ANOVA followed by Tukey's post hoc test

butyrate, within a wide range of doses adopted in different disease contexts, was effective in reducing AP and showed no harmful effects, indicating its potential application for prophylaxis for AP. The wide range of effective doses of sodium butyrate is likely to be related to the different disease phenotypes. Exogenous butyrate, provide by dietary supplementation, can be absorbed by colonocytes and then delivered to peripheral tissues to treat non-intestinal diseases

(McNabney & Henagan, 2017). Thus, the biological gradient for butyrate falls from the gut lumen to the periphery and leads to differing tissue butyrate exposure (Le Poul et al., 2003).

Infiltration of inflammatory immune cells and the resultant release of pro-inflammatory mediators play a pivotal role in the pathogenesis of AP (Gukovskaya et al., 2017). Our data suggested that butyrate limited the recruitment of neutrophils in the pancreas during AP. Similar

observations have been reported in acute lung injury (Li et al., 2018) and in mice with colitis (Simeoli et al., 2017), where butyrate treatment reduced the infiltration of neutrophils into injured tissues. Furthermore, we observed that butyrate facilitated the polarization of macrophages to the reparative M2 phenotype in the pancreas, which is important in resolving inflammatory responses during pancreatitis (Xue et al., 2015). Consistent with our findings, Ji et al. (2016) demonstrated that butyrate could ameliorate DSS-induced colitis by enhancing the polarization of M2 macrophage. Therefore, butyrate exerts its protective effects on AP in part by inhibiting infiltration of neutrophils and facilitating M2 macrophage polarization.

Transcription factors, such as NF- κ B, AP1, STAT1, and STAT3, regulate activation of immune cells and production of cytokines during AP (Chen et al., 2011; Gukovskaya et al., 2017; Robinson, Vona-Davis, Riggs, Jackson, & McFadden, 2006). Butyrate prophylaxis markedly decreased the phosphorylation of NF- κ B p65, AP1, STAT1, and STAT3 in pancreas, as well as NF- κ B p65 and AP1 in colon, but failed to suppress phosphorylation of STAT1 or STAT3 in colon, suggesting divergent tissue-specific regulatory effects of butyrate. In addition, the NLRP3 inflammasome has been implicated in the pathogenesis of AP (Hoque et al., 2011), and its activation is directly regulated by transcription factors including NF- κ B, AP1, and STAT1. Specifically, there are two NF- κ B binding sites in the NLRP3 promoter region (1434 to 1113; Qiao, Wang, Qi, Zhang, & Gao, 2012), and activated NF- κ B translocates to the nucleus and triggers the transcription of NLRP3 and pro-forms of inflammasome-related cytokines (Bauernfeind et al., 2009; Liu, Zhang, Joo, & Sun, 2017). AP1 is also a transcriptional activator, which mediates the gene induction of NLRP3 by binding with the promoter region of NLRP3 (Yang et al., 2014). In the study of Wang et al. (2017), phosphorylation of STAT1, a downstream effector of JAK1, was blocked by JAK1 knockdown, and subsequently, NLRP3 inflammasome activation is inhibited in human THP-1 derived macrophages. In our study, concomitant with down-regulated phosphorylation of NF- κ B p65, STAT1, and AP1, the activation of NLRP3 inflammasome in pancreas and colon was suppressed by butyrate, and NLRP3 inhibition has been shown to prevent the progression of pancreatitis (Kanak et al., 2017). In addition, the inhibitory effects of butyrate on NLRP3 inflammasome were further confirmed in peritoneal macrophages. Earlier work had also confirmed the anti-inflammatory activities of butyrate in adipocytes (Wang et al., 2015) and Caco-2 cells (Feng, Wang, Wang, Huang, & Wang, 2018) by inhibiting NLRP3 inflammasome. Collectively, these findings imply that butyrate partly protects against AP by suppressing NLRP3 inflammasome activation via modulating its upstream transcription factors.

Mechanistically, butyrate may regulate transcription factor expression and signal transduction pathways epigenetically by inhibiting HDACs, specifically class I/II HDACs (Chang et al., 2014; Chen et al., 2018). Indeed, we found that butyrate selectively inhibited HDAC1 expression and enhanced histone 3 acetylation levels at H3K9, H3K14, H3K18, and H3K27 loci in pancreas but did not affect histone acetylation at these loci in colon, suggesting that butyrate acts as an HDAC inhibitor to protect pancreatic but not colon injury. Consistent with our findings, Hartman,

Wetterholm, Thorlacijs, and Regnér (2015) suggested that HDAC inhibitors decreased pancreatic amylase levels and gene expression of CCL2, IL-6, and IL-1 β . Furthermore, our Co-IP analysis showed that down-regulation of HDAC1 by butyrate blocked the activation of STAT1 and AP1 in pancreas during AP, and data from peripheral macrophages also confirmed the inhibitory effects of butyrate on HDAC1 expression and AP1/STAT1 activation during the inflammatory response. In terms of the regulation by butyrate of the interaction between HDAC1 and transcription factors, other studies have shown that HDAC1 controls STAT1 activity (Göschl et al., 2018) and is involved in STAT1 transcriptional regulation by binding to STAT1 promoter (Ivanov, Salnikow, Ivanova, Bai, & Lerman, 2006). Therefore, HDAC1 inhibition by butyrate might reduce the recruitment of HDAC1 to STAT1 promoter and consequently decreased phosphorylation of STAT1. Moreover, Sanna and Galletti (2018) support that HDAC1 inhibitors block AP1 transcription, which contributes to antinociceptive activity in a neuropathic pain model. These findings, together with the suppressed NLRP3 inflammasome activation, provide the first evidence that butyrate protects against pancreatic inflammation during AP through inhibiting activation of the NLRP3 inflammasome, mediated by a HDAC1-STAT1/AP1 pathway.

Aside from functioning as an HDAC inhibitor, another known mechanism of butyrate is signalling through GPCRs, particularly GPR109A and GPR41 (Tan et al., 2014; Thorburn, Macia, & Mackay, 2014). Intriguingly, we observed that butyrate up-regulated the expression of GPR109A in colon, but not in pancreas. This observation, on one hand, is likely to reflect the tissue-specific expression of GPCRs, as GPR109A is highly expressed on the lumen-facing apical membrane of colonic and intestinal epithelial cells (Elangovan et al., 2014; Koh et al., 2016; Thorburn et al., 2014). On the other hand, butyrate has also been shown to activate GPR109A at millimolar concentrations (EC_{50} , 1.6 mM) and this short chain fatty acid is produced in large quantities (10–20 mM) by bacterial fermentation of dietary fibres in the colon (Koh et al., 2016). However, such concentrations are not likely to be achieved in the systemic circulation (our data showed concentrations of 63–99 μ M, Figure 1g) and in the pancreas (0.02–0.16 μ mol·g⁻¹, Figure 1g) during AP. Thus, the beneficial effects driven by butyrate activating GPR109A are more likely to have occurred in the colon during AP. In support of this possibility, the activation of GPR109A by butyrate has been documented earlier to maintain gut homeostasis by suppressing colonic inflammation (Lee et al., 2013; Macia et al., 2015; Singh et al., 2014). Also, we observed that along with GPR109A activation, butyrate inhibited NF- κ B p65 phosphorylation and downstream NLRP3 inflammasome activation in the colon (Lee et al., 2013; Sivaprakasam, Prasad, & Singh, 2016), and this may account for attenuation of AP-associated colonic inflammation. In addition, a GPR109A-mediated mechanism was confirmed by impaired gut barrier function, increased NLRP3 inflammasome activation, and partly diminished protection against AP in GPR109A^{-/-} mice, and this implies that butyrate-induced suppression of colonic inflammation through GPR109A signalling could alleviate pancreatic damage retroactively.

Collectively, our data demonstrate that butyrate prophylaxis attenuated pancreatic damage and associated intestinal injury during AP by several different mechanisms: In the pancreas, butyrate exerted anti-inflammatory effects by acting as an HDAC inhibitor inhibiting the interaction between HDAC1 and AP1, and STAT1 and subsequently suppressing NLRP3 inflammasome and infiltration of immune cells. In the colon, butyrate inhibited the phosphorylation of NF- κ B p65 and AP1 and their downstream NLRP3 inflammasome activation in a GPR109A-dependent manner. Improved intestinal homeostasis by butyrate through GPR109A facilitates attenuation of pancreatic inflammation. Our study provides novel insights into the anti-inflammatory mechanisms of butyrate in AP, and butyrate prophylaxis represents a potential strategy for AP prevention.

ACKNOWLEDGEMENTS

The work was supported by funds from the National Natural Science Foundation of China (Grants 81870439, 91642114, 31570915, 81573420, 31900644, 81973322, National Youth 1000 Talents Plan), Jiangsu Province Recruitment Plan for High-level, Innovative and Entrepreneurial Talents, the Fundamental Research Funds for the Central Universities (Grant JUSRP11866), National First-class Discipline Program of Food Science and Technology (Grant JUFSTR20180103), Wuxi Social Development Funds for International Science & Technology Cooperation (Grant WX0303B010518180007PB), China Postdoctoral Science Foundation (Grant 2018M642170), Natural Science Foundation of Jiangsu Province, China (Grant BK20180619), Jiangsu Planned Projects for Postdoctoral Research Funds (Grant 2018K238C), Collaborative Innovation Center of Food Safety and Quality Control in Jiangsu Province.

AUTHOR CONTRIBUTIONS

X.F., X.P., F.W., H.L., C.W., J.L., and X.T. performed the experiments and analysed the data. W.N. and W.L. assisted the experiments. X.P. and X.F. drafted the manuscript. J.S. and L.-L.P. designed the research project, supervised the experiments, and critically reviewed the manuscript.

CONFLICT OF INTEREST

The authors declare no conflicts of interest.

DECLARATION OF TRANSPARENCY AND SCIENTIFIC RIGOUR

This Declaration acknowledges that this paper adheres to the principles for transparent reporting and scientific rigour of preclinical research as stated in the *BJP* guidelines for [Design & Analysis](#), [Immunoblotting and Immunochemistry](#), and [Animal Experimentation](#), and as recommended by funding agencies, publishers, and other organizations engaged with supporting research.

ORCID

Jia Sun  <https://orcid.org/0000-0002-4874-1305>

REFERENCES

- Alexander, S. P. H., Christopoulos, A., Davenport, A. P., Kelly, E., Marrion, N. V., Peters, J. A., ... CGTP Collaborators (2017). The Concise Guide to PHARMACOLOGY 2017/18: G protein-coupled receptors. *British Journal of Pharmacology*, 174, S17–S129. <https://doi.org/10.1111/bph.13878>
- Alexander, S. P. H., Fabbro, D., Kelly, E., Marrion, N. V., Peters, J. A., Faccenda, E., ... CGTP Collaborators (2017). The Concise Guide to PHARMACOLOGY 2017/18: Enzymes. *British Journal of Pharmacology*, 174, S272–S359. <https://doi.org/10.1111/bph.13877>
- Alexander, S. P. H., Kelly, E., Marrion, N. V., Peters, J. A., Faccenda, E., Harding, S. D., ... CGTP Collaborators (2017). The Concise Guide to PHARMACOLOGY 2017/18: Other proteins. *British Journal of Pharmacology*, 174, S1–S16. <https://doi.org/10.1111/bph.13882>
- Alexander, S. P. H., Roberts, R. E., Broughton, B. R. S., Sobey, C. G., George, C. H., Stanford, S. C., ... Ahluwalia, A. (2018). Goals and practicalities of immunoblotting and immunohistochemistry: A guide for submission to the British Journal of Pharmacology. *British Journal of Pharmacology*, 175(3), 407–411. <https://doi.org/10.1111/bph.14112>
- Arpaia, N., Campbell, C., Fan, X., Dikly, S., van der Veen, J., deRoos, P., ... Rudensky, A. Y. (2013). Metabolites produced by commensal bacteria promote peripheral regulatory T-cell generation. *Nature*, 504(7480), 451–455. <https://doi.org/10.1038/nature12726>
- Bauernfeind, F. G., Horvath, G., Stutz, A., Alnemri, E. S., MacDonald, K., Speert, D., ... Latz, E. (2009). Cutting edge: NF- κ B activating pattern recognition and cytokine receptors license NLRP3 inflammasome activation by regulating NLRP3 expression. *Journal of Immunology*, 183(2), 787–791. <https://doi.org/10.4049/jimmunol.0901363>
- Chang, P., Hao, L., Offermanns, S., & Medzhitov, R. (2014). The microbial metabolite butyrate regulates intestinal macrophage function via histone deacetylase inhibition. *Proceedings of the National Academy of Sciences*, 111(6), 2247–2252. <https://doi.org/10.1073/pnas.1322269111>
- Chen, P., Huang, L., Zhang, Y., Qiao, M., Yao, W., & Yuan, Y. (2011). The antagonist of the JAK-1/STAT-1 signaling pathway improves the severity of cerulein-stimulated pancreatic injury via inhibition of NF- κ B activity. *International Journal of Molecular Medicine*, 27(5), 731–738. <https://doi.org/10.3892/ijmm.2011.632>
- Chen, S., Ye, J., Chen, X., Shi, J., Wu, W., Lin, W., ... Li, S. (2018). Valproic acid attenuates traumatic spinal cord injury-induced inflammation via STAT1 and NF- κ B pathway dependent of HDAC3. *Journal of Neuroinflammation*, 15(1), 150. <https://doi.org/10.1186/s12974-018-1193-6>
- Curtis, M. J., Alexander, S., Cirino, G., Docherty, J. R., George, C. H., Gienbycz, M. A., ... Ahluwalia, A. (2018). Experimental design and analysis and their reporting II: Updated and simplified guidance for authors and peer reviewers. *British Journal of Pharmacology*, 175(7), 987–993. <https://doi.org/10.1111/bph.14153>
- Elangovan, S., Pathania, R., Ramachandran, S., Ananth, S., Padia, R., Lan, L., ... Thangaraju, M. (2014). The niacin/butyrate receptor GPR109A suppresses mammary tumorigenesis by inhibiting cell survival. *Cancer Research*, 74(4), 1166–1178. <https://doi.org/10.1158/0008-5472.CAN-13-1451>
- Feng, Y., Wang, Y., Wang, P., Huang, Y., & Wang, F. (2018). Short-chain fatty acids manifest stimulative and protective effects on intestinal barrier function through the inhibition of NLRP3 inflammasome and autophagy. *Cellular Physiology and Biochemistry*, 49(1), 190–205. <https://doi.org/10.1159/000492853>
- Ginter, T., Bier, C., Knauer, S., Sughra, K., Hildebrand, D., Münz, T., ... Krämer, O. H. (2012). Histone deacetylase inhibitors block IFN γ -induced STAT1 phosphorylation. *Cellular Signalling*, 24(7), 1453–1460. <https://doi.org/10.1016/j.cellsig.2012.02.018>
- Gorelick, F. S., & Lerch, M. M. (2017). Do animal models of acute pancreatitis reproduce human disease? *Cellular and Molecular Gastroenterology*

- and *Hepatology*, 4(2), 251–262. <https://doi.org/10.1016/j.jcmgh.2017.05.007>
- Göschl, L., Preglej, T., Hamminger, P., Bonelli, M., Andersen, L., Boucheron, N., ... Ellmeier, W. (2018). A T cell-specific deletion of HDAC1 protects against experimental autoimmune encephalomyelitis. *Journal of Autoimmunity*, 86, 51–61. <https://doi.org/10.1016/j.jaut.2017.09.008>
- Grimaldi, G., Nocerino, R., Paparo, L., Cosenza, L., Aitoro, R., Trinchese, G., ... Berni Canani, R. (2016). The potential immunonutritional role of parmigiano reggiano cheese in children with food allergy. *Progress in Nutrition*, 18(1), 3–7.
- Gukovskaya, A. S., Gukovsky, I., Algul, H., & Habtezion, A. (2017). Autophagy, inflammation, and immune dysfunction in the pathogenesis of pancreatitis. *Gastroenterology*, 153(5), 1212–1226. <https://doi.org/10.1053/j.gastro.2017.08.071>
- Guo, Y., Xiao, Z., Wang, Y., Yao, W., Liao, S., Yu, B., ... Gong, Q. (2018). Sodium butyrate ameliorates streptozotocin-induced type 1 diabetes in mice by inhibiting the HMGB1 expression. *Frontiers in Endocrinology*, 9, 630. <https://doi.org/10.3389/fendo.2018.00630>
- Harding, S. D., Sharman, J. L., Faccenda, E., Southan, C., Pawson, A. J., Ireland, S., ... NC-IUPHAR (2018). The IUPHAR/BPS Guide to PHARMACOLOGY in 2018: Updates and expansion to encompass the new guide to IMMUNOPHARMACOLOGY. *Nucleic Acids Research*, 46, D1091–D1106. <https://doi.org/10.1093/nar/gkx1121>
- Hartman, H., Wetterholm, E., Thorlacius, H., & Regnér, S. (2015). Histone deacetylase regulates trypsin activation, inflammation, and tissue damage in acute pancreatitis in mice. *Digestive Diseases and Sciences*, 60(5), 1284–1289. <https://doi.org/10.1007/s10620-014-3474-y>
- He, Y., Wu, C., Li, J., Li, H., Sun, Z., Zhang, H., ... Sun, J. (2017). Inulin-type fructans modulates pancreatic-gut innate immune responses and gut barrier integrity during experimental acute pancreatitis in a chain length-dependent manner. *Frontiers in Immunology*, 8, 1209. <https://doi.org/10.3389/fimmu.2017.01209>
- Hoque, R., Sohail, M., Malik, A., Sarwar, S., Luo, Y., Shah, A., ... Mehal, W. (2011). TLR9 and the NLRP3 inflammasome link acinar cell death with inflammation in acute pancreatitis. *Gastroenterology*, 141(1), 358–369. <https://doi.org/10.1053/j.gastro.2011.03.041>
- Ivanov, S. V., Salnikow, K., Ivanova, A. V., Bai, L., & Lerman, M. I. (2006). Hypoxic repression of STAT1 and its downstream genes by a pVHL/HIF-1 target DEC1/STRA13. *Oncogene*, 26, 802.
- Ji, J., Shu, D., Zheng, M., Wang, J., Luo, C., Wang, Y., ... Qu, H. (2016). Microbial metabolite butyrate facilitates M2 macrophage polarization and function. *Scientific Reports*, 6, 24838. <https://doi.org/10.1038/srep24838>
- Kanak, M. A., Shahbazov, R., Yoshimatsu, G., Levy, M. F., Lawrence, M. C., & Naziruddin, B. (2017). A small molecule inhibitor of NF- κ B blocks ER stress and the NLRP3 inflammasome and prevents progression of pancreatitis. *Journal of Gastroenterology*, 52(3), 352–365. <https://doi.org/10.1007/s00535-016-1238-5>
- Kilkenny, C., Browne, W., Cuthill, I. C., Emerson, M., & Altman, D. G. (2010). Animal research: Reporting in vivo experiments: The ARRIVE guidelines. *British Journal of Pharmacology*, 160(7), 1577–1579. <https://doi.org/10.1111/j.1476-5381.2010.00872.x>
- Koh, A., De Vadder, F., Kovatcheva-Datchary, P., & Bäckhed, F. (2016). From dietary fiber to host physiology: Short-chain fatty acids as key bacterial metabolites. *Cell*, 165(6), 1332–1345. <https://doi.org/10.1016/j.cell.2016.05.041>
- Laserna-Mendieta, E., Clooney, A., Carretero-Gomez, J., Moran, C., Sheehan, D., Nolan, J., ... Claesson, M. J. (2018). Determinants of reduced genetic capacity for butyrate synthesis by the gut microbiome in Crohn's disease and ulcerative colitis. *Journal of Crohn's & Colitis*, 12(2), 204–216. <https://doi.org/10.1093/ecco-jcc/jjx137>
- Le Poul, E., Loison, C., Struyf, S., Springael, J. Y., Lannoy, V., Decobecq, M. E., ... Detheux, M. (2003). Functional characterization of human receptors for short chain fatty acids and their role in polymorphonuclear cell activation. *The Journal of Biological Chemistry*, 278(28), 25481–25489. <https://doi.org/10.1074/jbc.M301403200>
- Lee, C., Kim, B. G., Kim, J. H., Chun, J., Im, J. P., & Kim, J. S. (2017). Sodium butyrate inhibits the NF-kappa B signaling pathway and histone deacetylation, and attenuates experimental colitis in an IL-10 independent manner. *International Immunopharmacology*, 51, 47–56. <https://doi.org/10.1016/j.intimp.2017.07.023>
- Lee, S., In, H., Kwon, M., Park, B., Jo, M., Kim, M., ... Kim, S. (2013). β -Arrestin 2 mediates G protein-coupled receptor 43 signals to nuclear factor- κ B. *Biological & Pharmaceutical Bulletin*, 36(11), 1754–1759. <https://doi.org/10.1248/bpb.b13-00312>
- Leus, N., Zwinderman, M., & Dekker, F. (2016). Histone deacetylase 3 (HDAC 3) as emerging drug target in NF- κ B-mediated inflammation. *Current Opinion in Chemical Biology*, 33, 160–168. <https://doi.org/10.1016/j.cbpa.2016.06.019>
- Li, N., Liu, X. X., Hong, M., Huang, X. Z., Chen, H., Xu, J. H., ... Gong, Q. (2018). Sodium butyrate alleviates LPS-induced acute lung injury in mice via inhibiting HMGB1 release. *International Immunopharmacology*, 56, 242–248. <https://doi.org/10.1016/j.intimp.2018.01.017>
- Liu, T., Zhang, L., Joo, D., & Sun, S. C. (2017). NF-kappaB signaling in inflammation. *Signal Transduction and Targeted Therapy*, 2, 17023. <https://doi.org/10.1038/sigtrans.2017.23>
- Macia, L., Tan, J., Vieira, A., Leach, K., Stanley, D., Luong, S., ... Mackay, C. R. (2015). Metabolite-sensing receptors GPR43 and GPR109A facilitate dietary fibre-induced gut homeostasis through regulation of the inflammasome. *Nature Communications*, 6, 6734. <https://doi.org/10.1038/ncomms7734>
- Maehara, T., Matsumoto, K., Horiguchi, K., Kondo, M., Iino, S., Horie, S., ... Hori, M. (2015). Therapeutic action of 5-HT₃ receptor antagonists targeting peritoneal macrophages in post-operative ileus. *British Journal of Pharmacology*, 172(4), 1136–1147. <https://doi.org/10.1111/bph.13006>
- McGrath, J. C., & Lilley, E. (2015). Implementing guidelines on reporting research using animals (ARRIVE etc.): New requirements for publication in BJP. *British Journal of Pharmacology*, 172(13), 3189–3193. <https://doi.org/10.1111/bph.12955>
- McNabney, S. M., & Henagan, T. M. (2017). Short chain fatty acids in the colon and peripheral tissues: A focus on butyrate, colon cancer, obesity and insulin resistance. *Nutrients*, 9(12), 1348. <https://doi.org/10.3390/nu9121348>
- Pan, L.-L., Li, J., Shamoon, M., Bhatia, M., & Sun, J. (2017). Recent advances on nutrition in treatment of acute pancreatitis. *Frontiers in Immunology*, 8, 762–762. <https://doi.org/10.3389/fimmu.2017.00762>
- Qiao, Y., Wang, P., Qi, J., Zhang, L., & Gao, C. (2012). TLR-induced NF- κ B activation regulates NLRP3 expression in murine macrophages. *FEBS Letters*, 586(7), 1022–1026. <https://doi.org/10.1016/j.febslet.2012.02.045>
- Robinson, K., Vona-Davis, L., Riggs, D., Jackson, B., & McFadden, D. (2006). Peptide YY attenuates STAT1 and STAT3 activation induced by TNF- α in acinar cell line AR42J. *Journal of the American College of Surgeons*, 202(5), 788–796. <https://doi.org/10.1016/j.jamcollsurg.2006.01.007>
- Rodriguez-Nicolas, A., Martínez-Chamorro, A., Jiménez, P., Matas-Cobos, A. M., Redondo-Cerezo, E., & Ruiz-Cabello, F. (2018). TH1 and TH2 cytokine profiles as predictors of severity in acute pancreatitis. *Pancreas*, 47(4), 400–405.
- Sanna, M. D., & Galeotti, N. (2018). The HDAC1/c-JUN complex is essential in the promotion of nerve injury-induced neuropathic pain through JNK signaling. *European Journal of Pharmacology*, 825, 99–106. <https://doi.org/10.1016/j.ejphar.2018.02.034>
- Sender, R., Dummer, A., Weiss, F. U., Krüger, B., Wartmann, T., Scharffetter-Kochanek, K., ... Mayerle, J. (2013). Tumour necrosis factor α secretion induces protease activation and acinar cell necrosis in acute experimental pancreatitis in mice. *Gut*, 62(3), 430–439. <https://doi.org/10.1136/gutjnl-2011-300771>

- Simeoli, R., Mattace Raso, G., Pirozzi, C., Lama, A., Santoro, A., Russo, R., ... Meli, R. (2017). An orally administered butyrate-releasing derivative reduces neutrophil recruitment and inflammation in dextran sulphate sodium-induced murine colitis. *British Journal of Pharmacology*, 174(11), 1484–1496. <https://doi.org/10.1111/bph.13637>
- Singh, N., Gurav, A., Sivaprakasam, S., Brady, E., Padia, R., Shi, H., ... Ganapathy, V. (2014). Activation of Gpr109a, receptor for niacin and the commensal metabolite butyrate, suppresses colonic inflammation and carcinogenesis. *Immunity*, 40(1), 128–139. <https://doi.org/10.1016/j.immuni.2013.12.007>
- Sivaprakasam, S., Prasad, P., & Singh, N. (2016). Benefits of short-chain fatty acids and their receptors in inflammation and carcinogenesis. *Pharmacology & Therapeutics*, 164, 144–151. <https://doi.org/10.1016/j.pharmthera.2016.04.007>
- Sun, J., Furio, L., Mecheri, R., van der Does, A. M., Lundeberg, E., Saveanu, L., ... Diana, J. (2015). Pancreatic β -cells limit autoimmune diabetes via an immunoregulatory antimicrobial peptide expressed under the influence of the gut microbiota. *Immunity*, 43(2), 304–317. <https://doi.org/10.1016/j.immuni.2015.07.013>
- Sun, Y., He, Y., Wang, F., Zhang, H., de Vos, P., & Sun, J. (2017). Low-methoxyl lemon pectin attenuates inflammatory responses and improves intestinal barrier integrity in caerulein-induced experimental acute pancreatitis. *Molecular Nutrition & Food Research*, 61(4), 1600885. <https://doi.org/10.1002/mnfr.201600885>
- Tan, J., McKenzie, C., Potamitis, M., Thorburn, A. N., Mackay, C. R., & Macia, L. (2014). The role of short-chain fatty acids in health and disease. *Advances in Immunology*, 121, 91–119. <https://doi.org/10.1016/B978-0-12-800100-4.00003-9>
- Thorburn, A. N., Macia, L., & Mackay, C. R. (2014). Diet, metabolites, and “western-lifestyle” inflammatory diseases. *Immunity*, 40(6), 833–842. <https://doi.org/10.1016/j.immuni.2014.05.014>
- Uhl, W., Warshaw, A., Imrie, C., Bassi, C., McKay, C. J., Lankisch, P. G., ... International Association of Pancreatology (2002). IAP guidelines for the surgical management of acute pancreatitis. *Pancreatology*, 2(6), 565–573. <https://doi.org/10.1159/000067684>
- Vieira, E., Leonel, A., Sad, A., Beltrão, N., Costa, T., Ferreira, T., ... Alvarez-Leite, J. I. (2012). Oral administration of sodium butyrate attenuates inflammation and mucosal lesion in experimental acute ulcerative colitis. *The Journal of Nutritional Biochemistry*, 23(5), 430–436. <https://doi.org/10.1016/j.jnutbio.2011.01.007>
- Vinolo, M. A., Rodrigues, H. G., Hatanaka, E., Sato, F. T., Sampaio, S. C., & Curi, R. (2011). Suppressive effect of short-chain fatty acids on production of proinflammatory mediators by neutrophils. *The Journal of Nutritional Biochemistry*, 22(9), 849–855. <https://doi.org/10.1016/j.jnutbio.2010.07.009>
- Wang, J. J., Wei, Z. K., Zhang, X., Wang, Y. N., Fu, Y. H., & Yang, Z. T. (2017). Butyrate protects against disruption of the blood-milk barrier and moderates inflammatory responses in a model of mastitis induced by lipopolysaccharide. *British Journal of Pharmacology*, 174, 3811–3822. <https://doi.org/10.1111/bph.13976>
- Wang, X., He, G., Peng, Y., Zhong, W., Wang, Y., & Zhang, B. (2015). Sodium butyrate alleviates adipocyte inflammation by inhibiting NLRP3 pathway. *Scientific Reports*, 5, 12676. <https://doi.org/10.1038/srep12676>
- Wang, Y., Han, Z., Fan, Y., Zhang, J., Chen, K., Gao, L., ... Wang, C. (2017). MicroRNA-9 inhibits NLRP3 inflammasome activation in human atherosclerosis inflammation cell models through the JAK1/STAT signaling pathway. *Cellular Physiology and Biochemistry*, 41(4), 1555–1571. <https://doi.org/10.1159/000470822>
- Watanabe, T., Kudo, M., & Strober, W. (2017). Immunopathogenesis of pancreatitis. *Mucosal Immunology*, 10(2), 283–298. <https://doi.org/10.1038/mi.2016.101>
- Xiao, A., Tan, M., Wu, L., Asrani, V., Windsor, J., Yadav, D., & Petrov, M. S. (2016). Global incidence and mortality of pancreatic diseases: A systematic review, meta-analysis, and meta-regression of population-based cohort studies. *The Lancet Gastroenterology & Hepatology*, 1(1), 45–55. [https://doi.org/10.1016/S2468-1253\(16\)30004-8](https://doi.org/10.1016/S2468-1253(16)30004-8)
- Xiong, H., Du, W., Zhang, Y., Hong, J., Su, W., Tang, J., ... Fang, J. Y. (2012). Trichostatin A, a histone deacetylase inhibitor, suppresses JAK2/STAT3 signaling via inducing the promoter-associated histone acetylation of SOCS1 and SOCS3 in human colorectal cancer cells. *Molecular Carcinogenesis*, 51(2), 174–184. <https://doi.org/10.1002/mc.20777>
- Xue, J., Sharma, V., Hsieh, M., Chawla, A., Murali, R., Pandol, S., & Habtezion, A. (2015). Alternatively activated macrophages promote pancreatic fibrosis in chronic pancreatitis. *Nature Communications*, 6, 7158. <https://doi.org/10.1038/ncomms8158>
- Yamawaki, Y., Yoshioka, N., Nozaki, K., Ito, H., Oda, K., Harada, K., ... Akagi, H. (2018). Sodium butyrate abolishes lipopolysaccharide-induced depression-like behaviors and hippocampal microglial activation in mice. *Brain Research*, 1680, 13–38. <https://doi.org/10.1016/j.brainres.2017.12.004>
- Yang, H., Xiao, L., Yuan, Y., Luo, X., Jiang, M., Ni, J., & Wang, N. (2014). Procyanidin B2 inhibits NLRP3 inflammasome activation in human vascular endothelial cells. *Biochemical Pharmacology*, 92(4), 599–606. <https://doi.org/10.1016/j.bcp.2014.10.001>
- Zhang, L., Xue, J., Jaffee, E. M., & Habtezion, A. (2013). Role of immune cells and immune-based therapies in pancreatitis and pancreatic ductal adenocarcinoma. *Gastroenterology*, 144(6), 1230–1240. <https://doi.org/10.1053/j.gastro.2012.12.042>

SUPPORTING INFORMATION

Additional supporting information may be found online in the Supporting Information section at the end of this article.

How to cite this article: Pan X, Fang X, Wang F, et al. Butyrate ameliorates caerulein-induced acute pancreatitis and associated intestinal injury by tissue-specific mechanisms. *Br J Pharmacol*. 2019;176:4446–4461. <https://doi.org/10.1111/bph.14806>